IOP Conference Series: Earth and Environmental Science

PAPER • **OPEN ACCESS**

Spatial distribution characteristics of landslides in Xiluodu Reservoir Area

To cite this article: Su Pengcheng *et al* 2020 *IOP Conf. Ser.: Earth Environ. Sci.* **570** 042015

IOP Conf. Series: Earth and Environmental Science **570** (2020) 042015 doi:10.1088/1755-1315/570/4/042015

Spatial distribution characteristics of landslides in Xiluodu Reservoir Area

Su Pengcheng[1,2] **, Ma Chun**[2*] **, Liu Jingjing**[1,2]**, Li Yong**[1,2]

[1] Institute of Mountain Hazards and Environment & Key Laboratory of Mountain Hazards and Surface Process,Chinese Academy of Sciences & Ministry of Water Conservancy, Chengdu, 610041, China
[2] University of Chinese Academy of Sciences, Beijing, 100049, China

***Corresponding author :** machun@imde.ac.cn

Abstract. There are many landslides in Xiluodu Reservoir Area. 161 landslides were interpreted to investigate. The key influential factors including the formation lithology, faults, rainfall, earthquake, reservoir water level and the Geodetecter methods was used to explore the relative impact of the factors and the interaction of the two factors on the spatial distribution of landslides. The results show that: (1) Due to the differences in the properties of different rock groups, the landslides show significant regional differences; (2) The landslides are mostly distributed in the range of 600~1200 m, 10°~40°, Ordovician-Silurian (O-S) strata, areas within 4 km of the fault, areas where the average annual rainfall is 800~900 mm and seismic peak ground acceleration of 0.15g; (3) There are 53 landslides affected by reservoir water. The effect is most obvious when the water level acts on the middle and front of the landslide. The effect time is gradually weakened with the annual deformation and stress adjustment; (4) Multi-factor interaction presents more clear relationship with the spatial distribution of landslides. The interaction of lithology and rainfall can explain 45.9 % of the spatial variation of landslides, which means that lithology and rainfall factors have the greatest influence on the spatial distribution of landslides. The results provide a certain basis for the prevention and control of landslides in Xiluodu Reservoir Area.

1. Introduction

Reservoir impoundment changes significantly the bank conditions and leads to the resurgence and deformation of slopes [1]. There are two aspects that require special attention: the impact of water level change on slope stability and the impact of landslide on reservoirs [1]. The landslide in the reservoir area had not received wide attention and extensive research until catastrophic landslide occurred in 1963 during the storage of Vaiont Reservoir in Italy [2]. Then researches become intense, including investigation on triggering factors [3-4], correlating the deformation rate to reservoir level [5], the impact of water level change on landslide stability [6-7] and long-term monitoring of slope deformation [8-9]. Riemer (1992) indicated that 85% of landslide occurred during construction or reservoir filling, or within 2 years after the completion [10]. Numerous landslides have been identified in many Chinese reservoir areas. For example, Qianjiangping landslide and Shuping landslide in Three Gorges Reservoir in Yangtze River [9,11]; Maoping landslide in Geheyan Reservoir in Qingjiang River [12]; Yumen landslide in Ertan Reservoir in Yalong River [13]; Jinjiang landslide in Baihetan Reservoir and Luojiazui landslide in Xiangjiaba Reservoir in Jinsha River [3,14].

After Xiluodu Hydropower Station was closed for impoundment on May 4, 2013, some old landslides resurrected in Xiluodu Reservoir Area (XRA). On April 24, 2014, Qinggangping landslide slipped during the storage of the reservoir, with a total volume of 2 million m^3. By the end of 2015, there were 60 bank deformation points. Among them, 21 large-scale landslides deformed, including Ganhaizi landslide, Yulinerzu landslide, and Huangtianba landslide [15]. This shows that reservoir operation will bring about great threat of landslide and it is necessary to find out the landslide distribution and the key influencing factors. The previous research mainly focuses on external inducing factors and internal controlling factors. Inducing factors such as rainfall, seismic activity, reservoir water and human engineering activities, especially the groundwater seepage and dynamic change of groundwater caused by rainfall and reservoir water have the greatest impact on the wading landslide stability [16-17]. The internal control factors are topography, stratigraphic lithology, and fault structure [18-20]. The research on landslides in XRA mainly focuses on single landslides. For example, Fan and Wang (2013) used $FLAC^{3D}$ to perform three-dimensional numerical displacement calculation and deformation analysis on Ganhaizi landslide [21]. Yin et al (2014) predicted the possible swell disasters caused by Ganhaizi landslide at 540 m dead water level and 600 m normal pool level by modifying submarine landslide surge source model of Gril and Watts (2005) [22,23]. The result was that surge generally did not pose a threat to Xiluodu Dam. Liu and Li (2018) studied the deformation and failure phenomena and evolution characteristics of Ganhaizi landslide and Yulinerzu landslide and discussed the deformation and failure characteristics of different landslides and the relationship between them and profile morphology [15]. Chen and Dai (2018) used three-years landslide monitoring data and reservoir water data to analyze the deformation of eight landslides and found that the sudden rise and fall of the reservoir water was the main reason for intensified landslide deformation [24].

Although studies have been conducted on individual or local landslides in XRA, there are few studies on the relationship between landslide distribution and the influencing factors. We identified the landslide data in XRA and combined with geographic detector method to study the single influence factors and factor interactions on the distribution of landslides, and to understand the distribution characteristics and control factors of landslides, providing a new idea for the study of landslide distribution in similar reservoir areas.

2. Study area

The Xiluodu Hydropower Station is 197.5 km away from Baihetan Hydropower Station, along the main stream of Jinsha River. Affected by the annual adjustment of the reservoir, normal pool level of XRA is 600 m, the dead water level is 540 m, and the total storage capacity is 12.8 billion m^3 [22]. The area is located in the transitional zone from Daliangshan area bordered by Yungui Plateau and Sichuan Basin to the Central Sichuan Basin, in high mountain with strong erosion. The topography is generally high in the west and low in the east, with considerable height difference. From the 30 m resolution DEM (Digital Elevation Model) data of XRA (http://www.gscloud.cn), it is known that the minimum elevation is 265 m and the highest is 3016 m, and the elevation of the mountain range mostly between 2000 m and 3000 m. The cutting depth of the valley is about 1500 m, forming a "V" shaped channel (Figure 1b). From the geological map (http://www.geodata.cn) of the 1:2.5 million research area, the lithology and fault distribution can be known. The strata are only missing Carboniferous, Devonian and Tertiary, and the remaining strata are exposed from Proterozoic to Quaternary. Paleozoic Cambrian (∈), Ordovician-Silurian (O-S) and Permian (P) are distributed in most sections and are the main strata, accounting for about 70%~80% of the area. Permian (P) is the main strata exposed in the dam area and the near-dam reservoir section. Mesozoic Triassic (T) is mainly distributed in the area above the abutment on both bank (Figure 1a). The lithological characteristics of the study area are shown in Table 1. The geological structure is dominated by east-north and south-north faults and folds. The main faults include Ebian-Jinyang fault zone and Lianfeng fault zone, and there are associated northwest trending faults (Figure 1b). Ebian-Jinyang fault zone is distributed on the left and right banks of the Shibantan to Daxing section about 23 km from the dam, with the left bank as the main part. Lianfeng fault zone is distributed on the right bank of Jinsha River from Huangping to the end of the reservoir. The northwest-trending fault has small scale and low zonation. According to 2015 "China Earthquake Parameter Zoning Map" (http://data.earthquake.cn),

IOP Conf. Series: Earth and Environmental Science **570** (2020) 042015 doi:10.1088/1755-1315/570/4/042015

the distribution map of seismic peak ground acceleration (PGA) in XRA is obtained (Figure 1c). Except for the PGA of 0.2 g in the limited range of the head and tail of the reservoir and 0.3 g in the extremely limited range of the tail of the reservoir, the central area is 0.1 g or 0.15 g. The average annual rainfall is between 790 mm and 940 mm, with distribution uneven in time and uniform in space. Most rainfall is concentrated from May to October, accounting for about 85%~90 % of the annual rainfall. Spatially, the area with an average annual rainfall greater than 900 mm is mainly located in the upstream of the tail of the reservoir and the dam site area, and the rainfall in most of the central part of the reservoir area is concentrated between 800 mm and 850 mm (Figure 1d).

Table 1. Lithology characteristics of the study area.

Stratigraphic age	Stratum	Brief description of main lithology
Quaternary	Q	alluvium, collapse, landslide accumulation, gravel, pebbles, silty clay
Triassic	T	argillaceous limestone, limestone, dolomitic limestone intercalated with sand shale
Permian	P	sandstone, siltstone, mudstone intercalated with limestone, gray-white bauxite and claystone at the bottom; basalt, sand shale and bauxite at the bottom
Devonian	D	sandstone, siltstone, mudstone, shale, sandy shale intercalated with marl, argillaceous limestone
Cambrian	∈	gray limestone, dolomite, gray-black dolomite limestone, limestone, argillaceous dolomite with gypsum; gray-green shale
Sinian	Z	conglomerate, glutenite, conglomerate sandstone, quartz sandstone, feldspar sandstone, tuffaceous sandstone, and purple shale
Ordovician-Silurian	O-S	argillaceous fine sandstone, quartz sandstone and shale, gray crystalline limestone, marl, black shale, sandy shale
Cretaceous-Paleogene	K-E	calcium-bearing mudstone intercalated with sandy marl, calcium-bearing fine-grained quartz sandstone
Nanhua-Sinian	Nh-Z	massive dolomite, dolomitic limestone, argillaceous dolomite, algae-bearing reef dolomite, gray-black flint bands or mass dolomite and dolomitic phosphorite
Sinian-Cambrian	Z-∈	Gray limestone, dolomite, gray-black dolomite limestone, limestone, argillaceous dolomite with gypsum; gray-green shale
Mesoproterozoic	Pt_2	gray-green and gray-black quartz sericite phyllite,

metamorphic sericite quartz siltstone

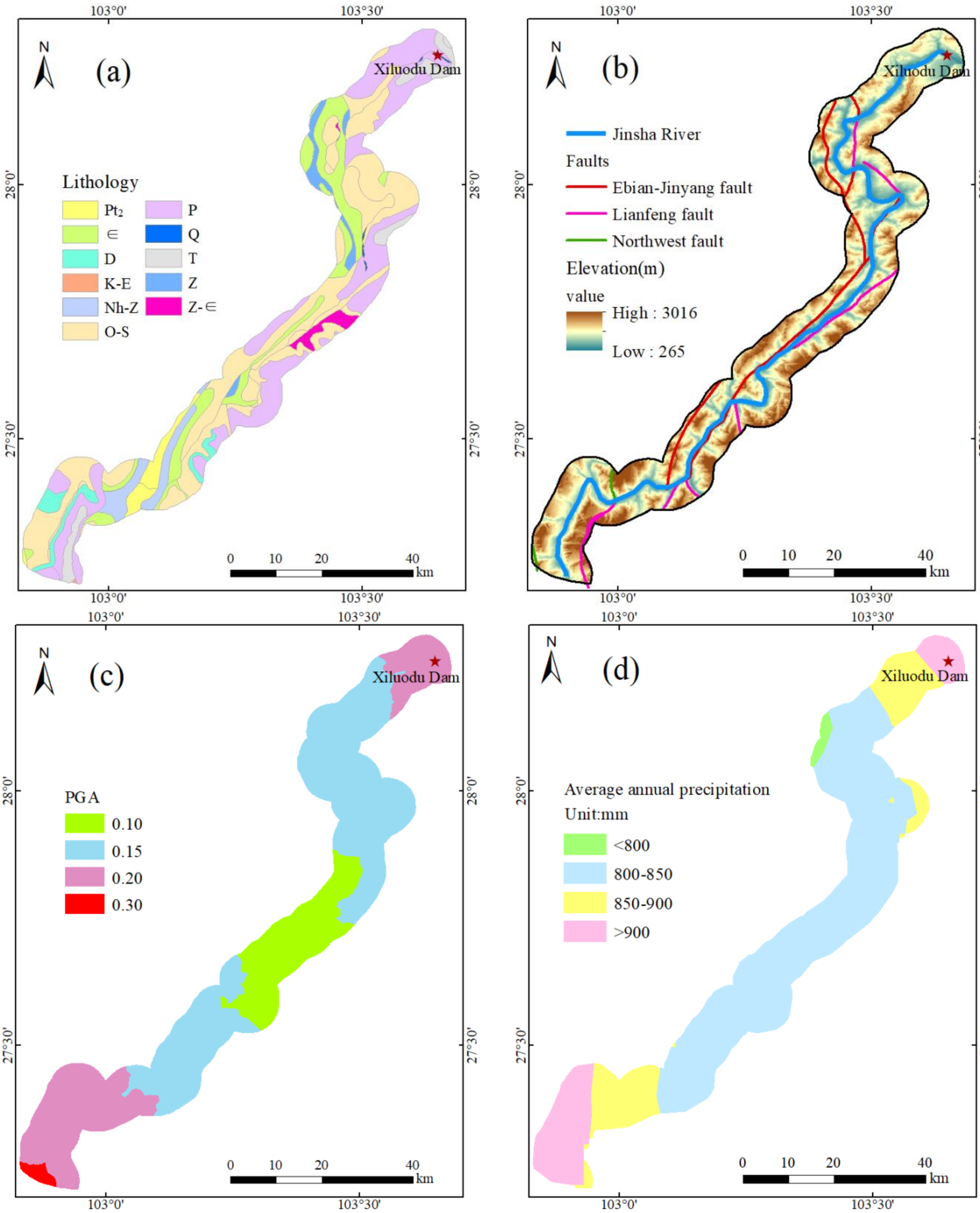

Figure 1. Distribution map of a) stratigraphic lithologic; b) faults; c) PGA; d) average annual rainfall in XRA.

3. Data sources and methods

3.1. Identification of landslide

Remote sensing technology is widely used in landslide disaster investigation in large-scale hydropower stations and other major projects [25]. The use of aerial photography for regional landslide disasters investigation mainly relies on the visual interpretation and interpretation of aerial photos, and a relatively mature method system has been formed [26]. In this paper, the digital elevation model (DEM) with a resolution of 2.5 m and orthophotos with resolution of 0.5 m are used to establish the topography of the three-dimensional scene, the interpretation of landslides were completed by combining the remote sensing interpretation method of geological information and interpretation signs of the landslides. The interpretative signs of landslides mainly include the following three aspects: (1) landform of landslides. It can be judged from a wide range of geomorphologic forms. For example, landslides are mostly developed in gentle slopes in canyons, shady slopes in watershed areas, and the intersection of the main and branch ditches and their sources where erosion basis changes rapidly. Judging from the shape, the back wall of the landslide is steep and looks like a chair. The landslide is generally in upwardly convex, showing a curved arc in the image; (2) material composition of the landslide; (3) environmental factors caused by the landslide, such as hydrological and vegetation abnormalities sign. Landslide and the surrounding geological body have obvious differences in hue, water system, texture, vegetation growth status. The vegetation on the landslide is younger than the surrounding vegetation. Abnormal river bends, local narrowing of river, wetlands and springs on the surface of the landslide, and linear exposure of groundwater in front of the slope are good interpretation signs for landslides. For landslides that once blocked rivers, drop water is often formed at the corresponding positions of the river, so the difference in the texture and color of the river can also be used as an indirect interpretation sign.

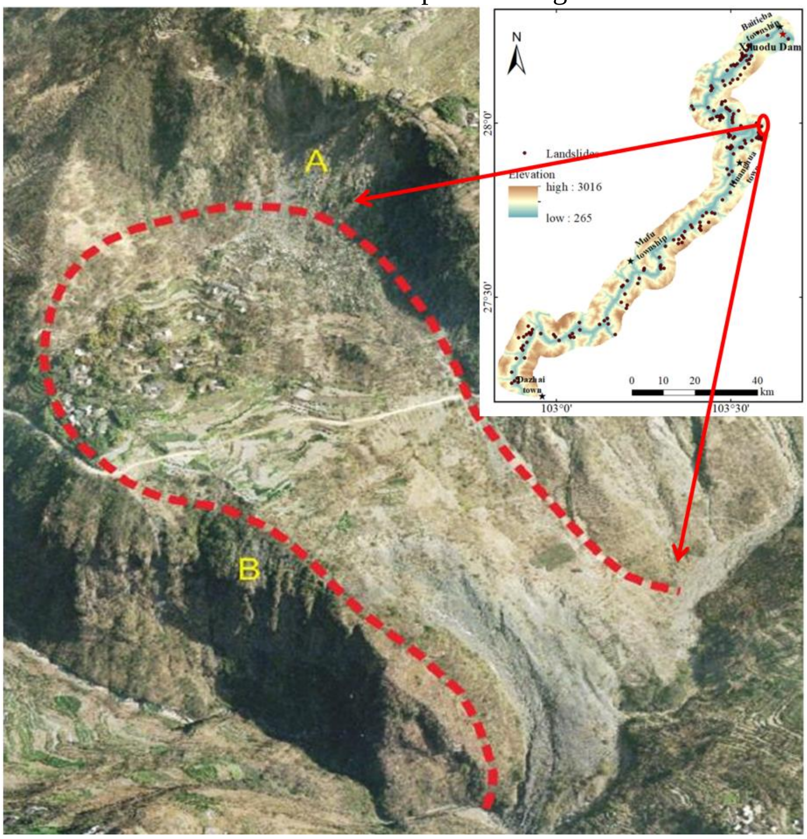

Figure 2. Aerial image of Guanyinmiao Landslide.

Taking the three-dimensional aerial image of Guanyinmiao landslide (Figure 2) as an example, it can be concluded that the trailing edge of landslide had a clear chair-like morphological feature. The posterior wall was a bedrock cliff with steep terrain, and the middle and rear part of landslide was gentler. Affected by the original terrain, the front was steeper. The front edge reached the bottom of the branch ditch and the posterior wall collapsed (the position shown in A), the collapse was mainly rock, and the landslide accumulation under the road was affected by erosion of the branch ditch, with obvious collapse and was in an unstable state. The left side of the lanslide is the bedrock cliff (the position shown in B). The occurrence of the rock layer could be identified according to the texture characteristics, which is relatively gentle. According to the exposed area of bedrock at the bottom of the sliding body, it can be considered that the landslide should be a high-shear outlet bedrock landslide. According to the interpretation results, combined with evaluation of reservoir bank stability of Xiluodu Hydropower Station in Jinsha River [27] and the on-site investigation review, it was finally determined that there were 161 landslides within 5 km on both banks of Jinsha River. We obtained the projected area of the landslide boundary and calculated the elevation difference between the front and rear edges of the landslide, from which the landslide volume can be derived by multiplying the projected area of the landslide [28]. According to "Technical Specifications for Design and Construction of Landslide Prevention Engineering" (DZ/T 0219-2006), it was known that there were 39 extra large landslides, 86 large landslides and 36 small and medium landslides in XRA (Figure 4).

3.2. Methods

On ArcGIS 10.2, the spatial pattern of influence factors is divided into several layers. Landslide density is used to explain landslide-prone areas [29], which is defined as the number of landslides on unit area of specific category:

$$F_i = \frac{N_{Li}}{A_i} \tag{1}$$

where F_i is the landslides density in the category *i*, N_{Li} is the number of landslides in the category *i*, and A_i is area of a specific category *i*.

We used the geographical detector method to analyse the relationship between landslide point density, *D* (we used the point density analysis function in the ArcGIS spatial analysis toolbox to calculate the point density, *D*. Then, the spatial distribution map of landslide density in XRA was calculated using 10×10 as the output size and 3 km×3 km as the neighbor, as shown in Figure 3a) and the influence factors, *X* in XRA. Geodetecter model is a statistical method developed around the hierarchical (class) heterogeneity or spatial differentiation of geographic phenomena [30]. It includes factor detector, risk detector, ecological detector and interaction detector. Factor detector can detect the dominant factors of landslide distribution, and interaction detector identifies how the interaction of factors enhanced or weakened the development of landslides. This method is described in detail in Wang et al (2010) [30]. The geographic detector method is based on the more similar the spatial distribution of the landslide point density *D* and the influence factor *X*, the greater the correlation between *D* and *X*. We use formula (2) to quantitatively describe the relationship between *D* and *X*:

$$q_{(X)} = 1 - \frac{\sum_{h=1}^{L} N_h \sigma_h^2}{N\sigma^2} \tag{2}$$

where *q* is the extent to which *D* is explained by the influence factor *X*; $h = 1, 2 \cdots, L$, is the number of strata of the influence factor X; N_h and N are respectively the number of sample units of strata *h* and XRA; σ_h^2 and σ_h are respectively point density variance of strata *h* and XRA. The value of *q* ranges from 0 to 1. The greater the value of *q*, the closer the relationship between the influence factor *X* and landslide point density *D*. If $q_{(X)} = 1$, the spatial distribution of *D* is completely determined by *X*; if $q_{(X)} = 0$, there is no association between *X* and *D*. This method is used to detect the spatial association of *X* and *D* rather than direct causality [31]. The interaction between the two different influence factors X_1 and X_2 is represented by the symbol ∩.The value of $q_{X_1 \cap X_2}$ indicates the ability of factor interactions to explain the distribution of *D*. By comparing the value of $q_{(X_1)}$, $q_{(X_2)}$ and $q_{X_1 \cap X_2}$, we can assess whether factor interactions will enhance or weaken the explanatory ability of factors to *D*. Therefore, geographical detector method can be used to study the relative influence of different influence factors and the interaction between the two factors on the spatial distribution of landslides in XRA.

The landslide spatial distribution is affected by many factors, which can be divided into seven catigories, including topography, geology, hydrology, soil, precipitation, land cover, and ground motion [32]. Deng and Wang proposed that the main internal control factors for the deformation and failure of the old landslide in XRA are stratum lithology and fault structure, and rainfall, reservoir water, earthquake and engineering influence are the main external factors[33]. Based on engineering geological environment characteristics and previous research results on landslides in XRA, we identified eight key influencing factors and divided them into the following five categories: topography (elevation, slope, aspect), geology (lithology, fault), climate (rainfall), seismicity (PGA), reservoir water. In terms of topography, slope and aspect were calculated by DEM grid analysis in the study area. With reference to the data discretization method proposed by Wang [30], elevation are divided into 9 levels: ≤600 m, 600~800 m, 800~1000 m, 1000~1200 m, 1200~1400 m, 1400~1600 m, 1600~1800 m, 1800~2000 m and >2000 m; slope is divided into 7 levels (Figure 3b); according to east, south, west, north, northeast, southeast, northwest, southwest and flat, aspect is divided into 9 levels (Figure 3c). For climatic factors, according to the dataset of "China Earth Cumulative Annual Value Data Set (1981~2010)" (http://data.cma.cn) of China Meteorological Data Network, 37 meteorological stations near the study area were selected. We use Kriging interpolation method in ArcGIS to obtain average annual rainfall in XRA. As the triggering factor, average annual rainfall is divided into 4 levels: <800 mm, 800~850 mm, 850~900 mm and >900 mm (Figure 1d). For earthquake factor, the PGA is divided into 4 levels: 0.1 g, 0.15 g, 0.2 g, and 0.3 g (Figure 1c). For faults, its impact on landslides depends on the distance [34-35], which falls into 6 levels by the distance from faults: <500 m, 500~1000 m, 1000~2000 m, 2000~3000 m, 3000~4000 m and >4000 m (Figure 3d). For stratigraphic lithology, there are eleven stratigraphic units in XRA, including Quaternary (Q), Triassic (T), Permian (P), Devonian (D), Cambrian (∈) , Sinian (Z), Ordovician-Siurian (O-S), Cretaceous-Paleogene (K-E), Nanhua-Sinian (Nh-Z), Sinian-Cambrian (Z -∈) and Mesoproterozoic (Pt_2) (Figure 1a). For the reservoir water factor, its influence range is only within the elevation range of 540～600 m, which plays a great role in the resurrection and deformation of the wading landslide within the elevation range [16-17].

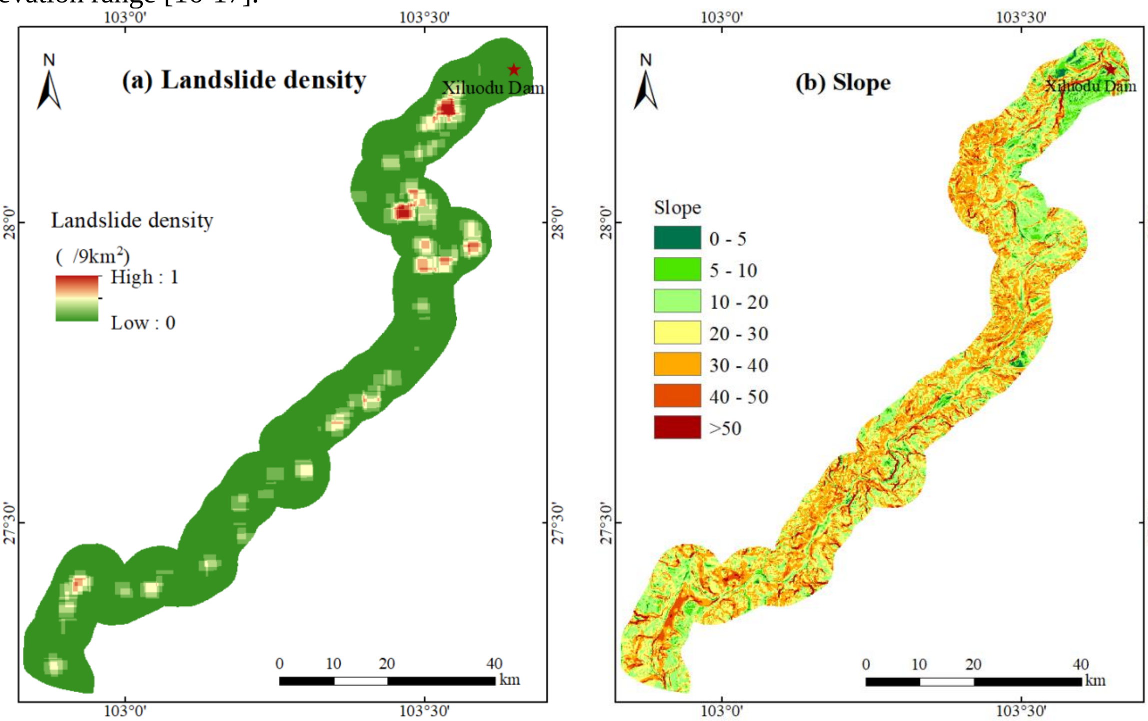

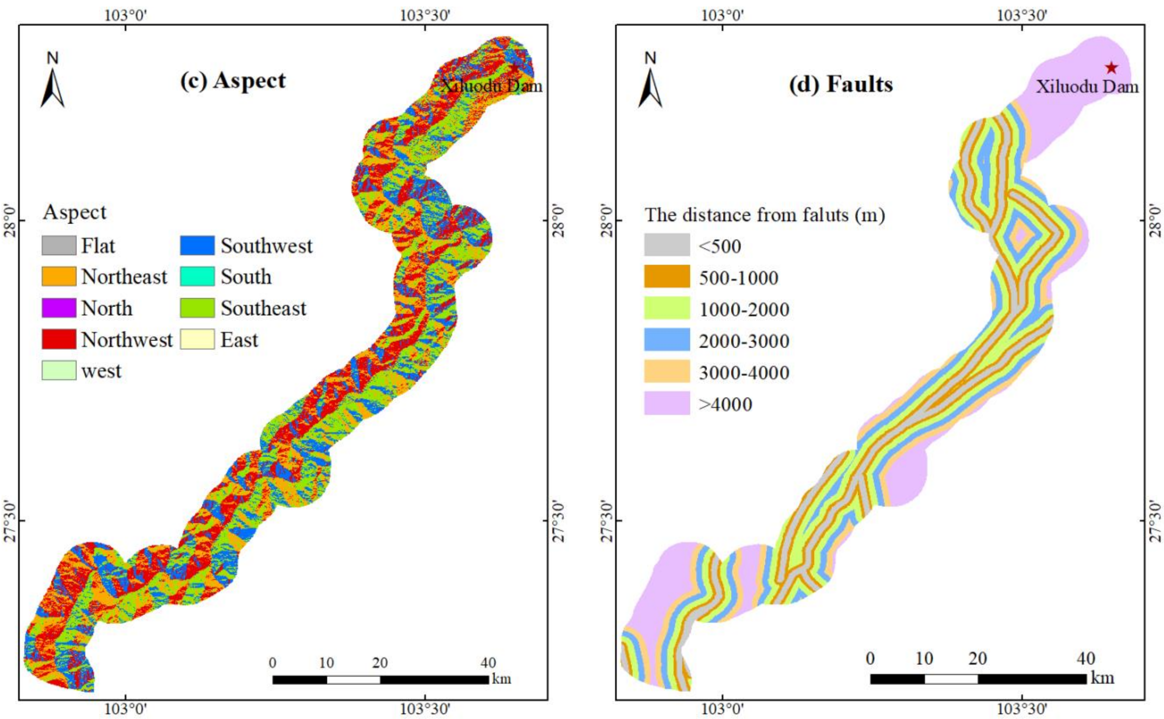

Figure 3. Distribution map of a) landslide density; b) slope; c) aspect; d) distance from fault in XRA.

4. Basic characteristics of landslide distribution

There are 161 landslides in XRA, of which 39 are extra large ones with a volume of more than 10 million m^3, accounting for 24.2 % of the total; 86 large landslides with a volume of 1 million to 10 million m^3, accounting for 53.4 %; There were 36 small and medium-sized landslides with a volume less than 1 million m^3, accounting for 22.4 %. The largest is Huanghua landslide with a volume of 61 million m^3 and a small scale of only tens of thousands m^3. The distribution of landslides is shown in Figure 4.

Landslides show obvious regional difference in each section (Figure 4). The main stream reservoir bank along Xiluodu dam to the tail of the reservoir is divided into a section every 10 km, and the distribution linear density (the number of landslides per kilometer) of each section is calculated. The macroscopic characteristics of the landslides development density along the main stream of Jinsha River can be obtained (Figure 5), and the distribution of landslides along the main reservoir bank can be divided into the following three characteristic zones:

The first section is Baitieba Township-Huanghua Town, about 40 km away from the dam, there are 86 landslides, accounting for 53.4%. The density is high, and it contains several concentrated areas of landslide, such as the reservoir bank of 10~20 km, 20~30 km, and 30~40 km away from the dam, among which the bank of 30~40 km has the highest line density of 4.3 /km. Typical extra large landslides in this section include Yangjiaping landslide, Ganhaizi landslide, Baisheng landslide, Yujiaao landslide, Yantangwan landslide, Huanghua landslide, etc.

The second section is from Huanghua Town to Mufu Township. The landslide linear density in this section has decreased compared with the first section and the overall distribution along the reservoir bank is relatively uniform. The maximum line density is 1.2/km. However, there are significant differences in the landslide distribution of the left and right bank. There are 4 landslides on the left bank of Jinsha River with small scales, and 31 on the right bank with large scales. Among them, 27 are large and extra large landslides, which is close to 8 times the number of landslides on the left bank. Songshuping landslide, Huilongcun landslide and Xiatianba landslide in this section are all typical large landslides. The third section is Mufu Township-Dazhai Town. Among them, the landslides in the reservoir bank section between 110 and 120 km away from the dam are most concentrated and there are many large and extra large landslides, of which the typical landslide is Niujiaowan landslide. In the tail section of the reservoir more than 120 km away from the dam, large and extra large landslides are mainly distributed on the left bank and only three on the right bank of Jinsha River.

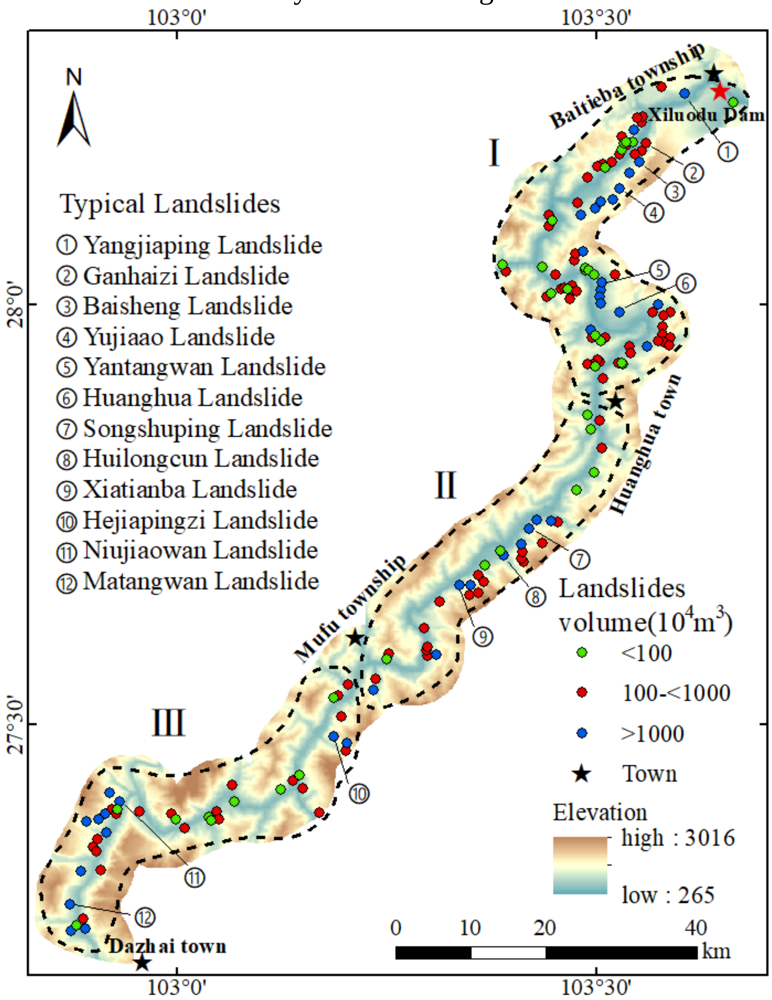

Figure 4. Spatial distribution of landslides in XRA.

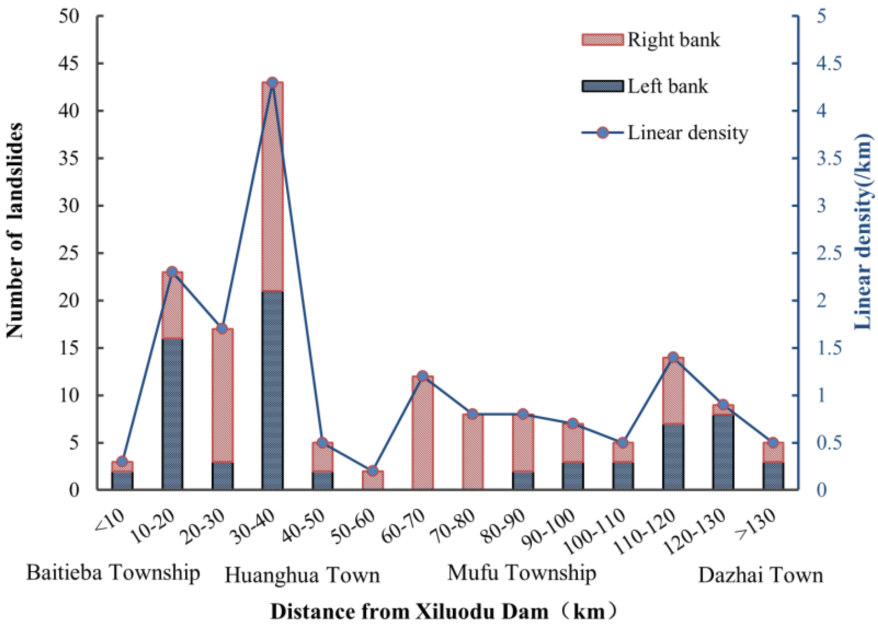

Figure 5. Distribution of landslide line density in XRA.

IOP Conf. Series: Earth and Environmental Science **570** (2020) 042015 doi:10.1088/1755-1315/570/4/042015

In general, landslide density is high in the north of Huanghua Town, while distribution density in the south of Huanghua Town is relatively uniform and not high. In some reservoir bank sections, the overall slope stability is good. For example, there are very few landslides in the reservoir bank of 50~60 km away from the dam, and only two small and medium landslides are developed on the right bank. Therefore, it can be concluded that landslide density shows significant local differences, and the density of the left and right bank or the upstream and downstream side of the small-scale reservoir bank section also shows local differences. For example, in the reservoir bank section of 50~80 km away from the dam, the landslides only develops on the right bank.

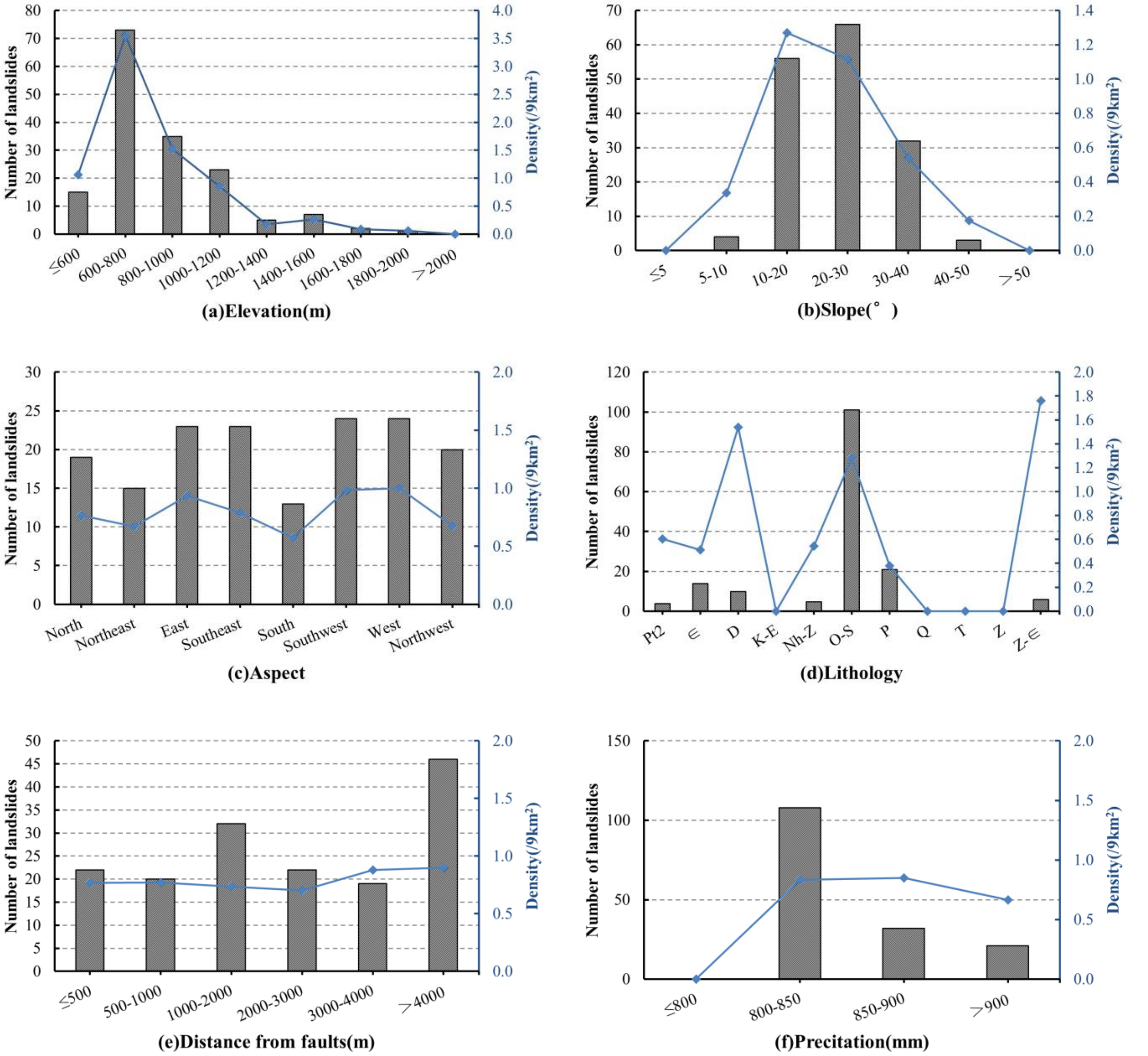

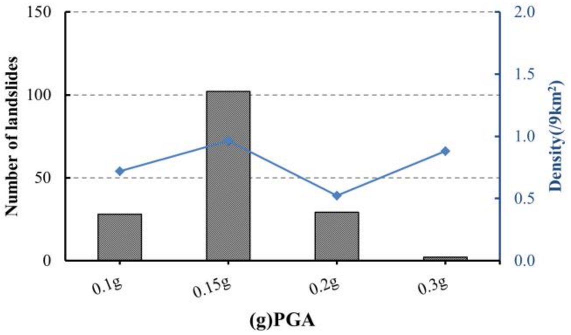

Figure 6. Relationship between landslide development density, quantity and influencing factors: a) elevation; b) slope; c) aspect; d) lithology; e) distance from fault; f) average annual rainfall; g) PGA.

5. Result

5.1. Individual factor

5.1.1.Elevation, slope and aspect.
Figure 6 shows the relationship between landslides distribution density and the various influence factors. Elevation will have a certain impact on landslides [36]. After the elevation exceeds 600 m, as the elevation increases, the number and distribution density of landslides generally decrease (Figure 6a). The landslides are mainly concentrated in the range of elevation from 600 m to 1200 m, and their density is greater than the average density of 0.80/9 km^2 in XRA, of which landslide density in the range of 600~800 m reaches 3.55/9 km^2. Only 9.3% of the landslides are located below the elevation of 600 m, which is the normal pool level, indicating that most of the landslides are affected by geological environment and rainfall in XRA. Previous studies have shown that slope has an important effect on the occurrence of landslides [37]. 75.8% of the landslides are distributed at slopes from 10° to 30°, and their density exceeds the average density of the study area by 0.80/9 km^2 (Figure 6b). 95.7% of the landslides are distributed at slopes of 10 °~40 °, so the slope of 10 °~40° is the main environment for the landslides development. Aspect affects both soil moisture retention and vegetion, which in turn affect soil strength and the susceptibility of landslides. Previous studies have shown that areas with south-facing slopes are landslide-porne in the Northern Hemisphere [35,38]. We found that the impact of ascept on landslides is not obvious, and the number and density of landslide vary little with aspect (Figure 6c).

5.1.2.Lithology and fault. Stratigraphic lithology affects
the strength and permeability of the materials that constitute the bank slope, and is an important factor for landslides [37]. The study area has the largest number of landslides distributed in O-S strata. The landslide distribution density is relatively high in Z-∈, D, and O-S strata, all of which are greater than 0.80/9 km^2 (Figure 6d). Among them, Z-∈ is the most prone to landslides (1.76/9 km^2). Faults destroy the rock mass structure and reduces the bank slope stability. 71.4% of the landslides occurred within 4 km of the fault (Figure 6e). Unlike other studies, in the range of 4 km from faults, with the increase of distance from faults, the number and density of landslides did not show a decreasing trend, and the density of landslides near the fault (<500 m) was lower than the average value, indicating that indicating that it had little effect on the reservoir bank landslide from the perspective of fault factor alone. In areas far away from faults, landslides development was affected by other factors.

Table 2. Division of engineering geological rock groups in XRA.

Rock group	Stratigraphic	Brief description of main lithology
Magmatic group	$P_2\beta$	Mainly composed of hard massive and thick layered basalt.
Carbonate group	P_1y、O_2、$\in_1+d$、$Z_b+\in_1m$、$\in_3e$、T_{1-2}	mainly composed of medium-thick layer to hard limestone and dolomite in massive.
Clastic group	Z_{a+b}、$\in_1q+c$、$\in_2x$、O_1、O_3+S、P_2x、T_1f+t	Sandstone, siltstone and shale with thin layer to interlayer structure.
Metamorpic group	Pt	Mainly composed of thin layered phyllite and slate with sandstone.
Loose deposits	Q	Mainly composed of loose soil deposits.

In order to further explore the influence of lithology, according to the formation, material composition and engineering geology of stratigraphic lithology, we divided the main geological rock layers into five groups: magmatic group, carbonate group, clastic group, metamorphic group and loose deposits. The main stratigraphic units are shown in Table 2. The distribution of each group is shown in Figure 7.

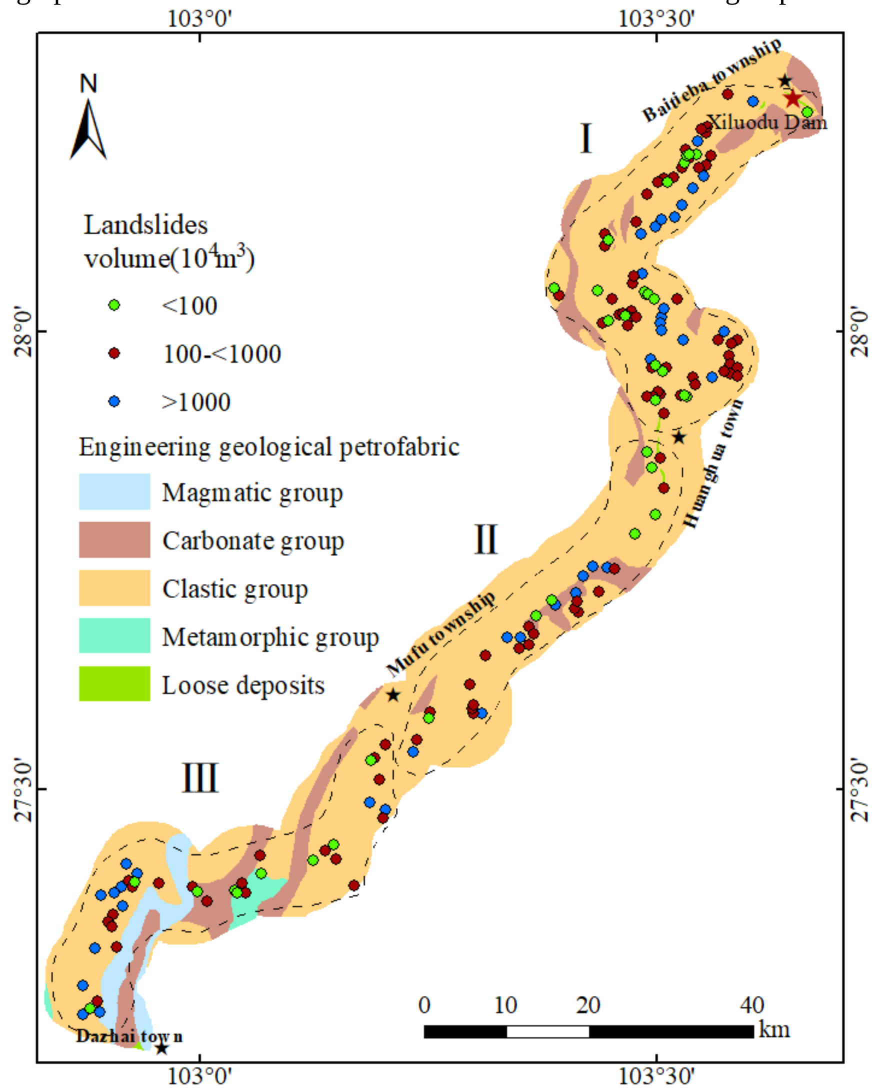

Figure 7. Distribution of engineering geological rock groups and landslides in XRA.

The correlation between landslide distribution and rock groups is shown in Table 3. Magmatic group is only distributed in Mufu Township-Dazhai Town section, and loose deposits are only distributed near the dam, and the area of the two groups is small where there is no landslide. Carbonate group has a distribution area of 13% and distribution density of 0.42/9 km^2. Metamorphic group is distributed in Mufu Township-Dazhai Town section, with an area of only 1.3%, but it is the rock group with the highest landslides density, which is 1.51/9 km^2. Clastic group is widely distributed in three sections, with area of 81.7%, where the number of landslides is the highest, reaching 146, accounting for 91.5%. Therefore, clastic group is the most important for landslide.

In summary, landslide density in each rock group is significantly different, which is closely related to physical and mechanical characteristics, water-rock interaction, weak interlayers and structural plane characteristics. Magmatic group is composed of hard massive and thick-bedded basalt rock groups. The basalt is hard and has high mechanical strength. The structural planes are mainly primary joints, quasi-levels and structural fissures. The bank slope is of good stability and gorge landform forms on high and steep reservoir bank, so there is no landslide in magmatic group.

In carbonate group, it is mainly composed of argillaceous limestone, limestone, and dolomite with shale. The limestone has a relatively pure texture and a high degree of karstification, and the argillaceous limestone and marlstone primary fissures can easily expand into solution crack or even karst collapse through dissolution, which further aggravates the development of joint fissures, providing a good channel for groundwater seepage. The underlying mudstone has a low permeability coefficient, which plays a role in water blocking. Groundwater flow is blocked and turned into a layered flow. The mudstone has certain expansibility and dry-wet cycle disintegration characteristics. Under long-term dissolution, sludging and softening, a potential slip surface is formed, and the rock mass is prone to rheology and deformation along the structural plane. For example, because its underlying muddy limestone and other weak interlayers were cut by the river water, Jinjiagou landslide deformed and destroyed under the action of gravity.

Table 3. Distribution characteristics of landslides in different engineering geological rock groups.

Rock group	Area (km^2)	Area ratio (%)	Number of landslides	Landslide quantity ratio (%)	Landslide density (/9 km^2)
Magmatic group	70.7	3.9	0	0	0
Carbonate group	235.0	13.0	11	6.8	0.42
Clastic group	1486.8	81.7	146	90.7	0.88
Metamorpic group	23.8	1.3	4	2.5	1.51
Loose deposits	3.1	0.1	0	0	0

Clastic group is composed of sandstone, siltstone and shale with thin layer to interlayer structure. The rock strength varies greatly, the sandstone with good permeability is high in strength. Shale is relatively low in strength, and has poor resistance to water immersion, easily softened and muddled in water. It is a typical softened rock and has a large distribution area. For example, landslide linear density in section of Baitieba Township-Huanghua Town is the highest, which occurs in soft rock layers such as siltstone or shale. Clastic group often contains a large amount of mudstone layers and soft structural (layer) surfaces of carbonaceous shale and coal seams. The existence of weak structural layers (surface) makes the slope more prone to instability. Almost all extra large landslides are distributed in this rock group. For example, Huanghua landslide is an extra large landslide caused by weak structural surfaces such as siltstone and shale. Therefore, the number of landslides is the highest and the density is relatively high in clastic group.

In metamorphic group, it is mainly composed of thin layered phyllite and slate with sandstone, with low strength, weak anti-weathering ability and poor rock integrity. It often forms a midslope terrain of about 40°, and the deformation and failure of slope are strong due to many short cracks and layer cutting. Metamorphic group is mainly concentrated in section of Mufu Township-Dazhai Town. Due to the undercutting of the river, a large area of unloading occurs during the formation of the slope. Slope deforms toward the free surface due to the unloading rebound. In addition to the poor rock integrity and the thin layer of phyllite and slate that are easily softened by flowing water and weathering, the slope deformation toward free surface is exacerbated, and deformation develops to a point where failure occurs, such as Zhandoushegou landslide and Damakou landslide.

5.1.3.Rainfall.

The main effect of rainfall on landslides is that rainfall infiltration increases the soil water content and pore water pressure and reduces the strength. The average annual rainfall in most areas is 800~850 mm (Figures 6f, 1d), but the area with the average annual rainfall of 850~900 mm has the highest density of landslides, 0.85/9 km^2. The maximum rainfall is mainly distributed in the head and tail of reservoir (Figure 1d), and it is not the area where average annual rainfall is greater, landslide density is greater. Further analysis shows that rainfall is converted into groundwater by infiltration and then interacts with rock and soil bodies on the bank slope to induce landslides. The interaction between groundwater and rock and soil bodies on slopes plays an important role in landslides.

5.1.4.Seismicity. Earthquakes can directly induce landslides. Wang (2011) studied the relationship between earthquake-induced landslides and PGA in Longmenshan earthquake area, and found that found that in areas with severe deformation and damage such as earthquake-induced collapse landslides, PGA is generally greater than 0.2 g; in areas with lighter collapse disasters have peak earthquakes. PGA is less than 0.2 g [39]. For this study area, 98.8 % of the landslides are distributed in the area where the PGA is less than 0.2 g, and 63.4% of the landslides are concentrated in the area where the PGA is 0.15 g, and the highest distribution density is 0.97/9 km^2. This indicates that the influence of PGA on the distribution of landslide is limited to a certain range. Beyond this range, the influence degree is relatively small. Therefore, the landslides may be more affected by local topography, geological environment, rainfall and other factors.

5.1.5.Reservoir water.

In May 2013, Xiluodu reservoir began to store water, and four slopes deformed when the storage reached 540 m in June, and five in October, 12 landslides occurred in this year, indicating that part of the landslides began to resurrect when the reservoir water level rose from 400 m to 540 m. From February to June 2014, only one slope deformed, which was the first decrease of water storage to 560 m. 600 m water storage began in June 2014. During the period from June to November, 3 slopes deformed [24]. After the reservoir water stabilized, the activity of landslide decreased. After that, the reservoir entered the stable operation stage, the overall number of landslide did not increase, and the stability trend increased.

Compared with Three Gorges Reservoir Area, the storage time of XRA to 600 m normal pool level was short, so the action time of reservoir water was short. In the early stage of impounding from May to October 2013, the number of landslide deformation was the highest with water level rising from 400 m to 540 m, and the impact of later water storage on landslides was gradually weakening. For example, during the period from June to November 2014, when water level reached 600 m, only 3 landslides deformed. Since then the number of landslide deformation has fallen to a minimum. The mechanical mechanism of reservoir water on the landslide is generally the seepage pressure effect caused by the hydraulic gradient difference between the inside and outside of the slope, and the second is the suspension weight loss effect of groundwater on the landslide. There are also deformations caused by the river cutting the foot of the slope, or the broken rock mass at the front edge is eroded and transported, which reduces the anti-sliding force. It can also be caused by the increase of the groundwater level of the slope, which leads to the effect of the water pressure of the confined aquifer on the roof, or the disintegration failure after experiencing dry-wet cycle conditions of water soaking and dehydration. This series of reservoir water mechanisms is closely related to the reservoir flooding ratio. The number of wading landslides in XRA reflects the extent to which the reservoir landslides are affected by the reservoir water, and the reservoir flooding ratio reflects the stability of the wading landslide. The wading degree of landslide can be characterized by reservoir flooding ratio (I), and its calculation formula is as follows:

$$I = \frac{h_N - h_L}{h_T - h_L} \times 100\% \tag{3}$$

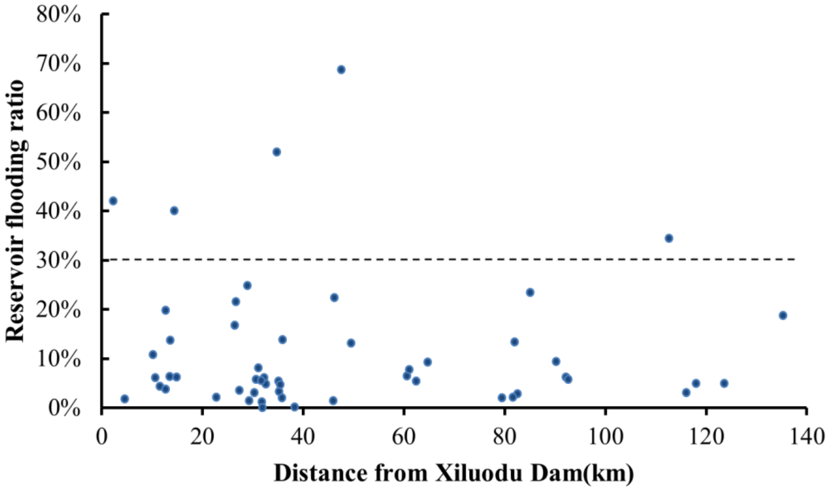

Figure 8. Distribution map of landslides inundate extent.

In the formula, h_L , h_T are respectively the elevation of the leading and trailing edge of the landslide (m). h_N is elevation of the normal pool level, 600 m. According to 0~30%, 30%~60%, 60%~100%, it is divided into three grades, which respectively represent the front, middle and rear of wading landslide. The inundation of 53 wading landslides is shown in Figure 8, which clearly shows that the number of wading landslides in section of Baitieba Township-Huanghua Town is the largest, accounting for 60.4% of the total wading landslides. The majority water flooded degree (98%) of landslide is under 60%, 90% of the wading landslides are below 30% of water flooded degree. This means that the reservoir water changes mainly in the middle and front of the landslide, and the main anti-slide section of the landslide is located in the middle and front part. If the landslide is controlled by a weak structural layer (surface), local deformation and damage are likely to occur under the action of reservoir water. Therefore, special attention should be paid to the stability of such wading landslides. Taking Ganhaizi landslide as an example, the upper part is a steep wall formed by basalt and Yangxin limestone, and the lower part is a gentle slope formed by Silurian mud shale, which is mainly controlled by the Silurian weak stratum. Under the action of reservoir water, mudstone and shale are prone to soften in water, which changed the mechanical properties of the rock and soil mass, resulting in a decrease in cohesion and a significant reduction in the shear strength of the lower soft layer. Then local deformation failure occurred.

5.2 Combined effect of influencing factors

Table 4 shows the q statistic of the influencing factors and their interactions with the spatial distribution of landslides, which is based on the geographic detector method. For a single factor, the q statistic for each factor range from 0.003 to 0.238, and the $p < 0.001$. For the interpretation capability, stratigraphic lithology has the strongest explanatory power in rock and environment factors; among topography factors, elevation has more important influence, and the aspect has the smallest influence; among the inducing factors, rainfall has a greater impact on the spatial distribution of landslides than earthquakes. The relative influence of the single factor on the spatial distribution of landslides obtained by the geographic detector method is consistent with the result in the individual factor analysis. Overall, the q statistic for lithology, rainfall, faults, and elevation ranges from 0.113 to 0.238. This value range indicated that these single factors are related to the spatial distribution of landslides, but their effects are limited. Further analysis of factor interaction effects on the spatial distribution of landslides showed that factor interactions are more closely related to the spatial distribution of landslides than individual factor. The top eight factor interactions with the greatest q statistics are listed in Table 4. The factor interactions can be divided into three categories: rainfall interactions with lithology, faults, elevation, and seismicity; lithology interactions with elevation, seismicity, and fault; fault and seismicity interactions. Among them, the interactions between lithology and rainfall have the greatest impact on the spatial distribution of landslides (q = 0.459), which can explain the spatial variation of landslide distribution of 45.9%. This suggests that in a particular stratigraphic lithological area, rainfall is more closely related to the spatial distribution of landslides. These areas are mainly located in section of Baitieba Township-Huanghua Town. This area not only has heavy rainfall, but also has a wide range of clastic group. According to the distribution of rock groups, the thin-to-layered sandstone, siltstone, mudstone and shale-based clastic groups provide the favourable conditions for landslides. The development of the structural plane provides a channel for rainfall infiltration and reservoir water infiltration. The lower mudstone and shale interlayers are prone to soften when they are exposed to water, resulting in a significant reduction in the shear strength of the weak structural layer and landslides. The interactions between rainfall and faults, elevation, and seismicity is also significant for the spatial distribution of landslides, with q statistics greater than individual factor. The interaction between lithology and elevation, seismicity and faults is also significant, and q statistic values are more than 0.3. Although the q statistic values of fault factor and seismicity factor are respectively 0.124 and 0.083, the interaction between fault and seismicity can explain 29.8% of the spatial distribution of the landslides.

Table 4. The q statistic of influencing factors and their interactions.

Factors	*q* statistic	Factor interaction	*q* statistic
Lithology	0.238	Lithology ∩ rainfall	0.459
Rainfall	0.178	Faults ∩ rainfall	0.425
Faults	0.124	Lithology ∩ elevation	0.328
Elevation	0.113	Lithology ∩ seismicity	0.326
Seismicity	0.083	Lithology ∩ faults	0.303
Slope	0.035	Faults ∩ seismicity	0.298
Aspect	0.003	Elevation ∩ rainfall	0.283
		Rainfall ∩ seismicity	0.243

6. Discussion

The spatial relationship between the landslide distribution points density and topography, geological environment, rainfall and seismicity factors was analyzed by geographic detector method. The *q* statistics of the interaction between rainfall and elevation, lithology, faults, seismicity and other factors are all greater than *q* statistic of individual factor, indicating that the causes of landslides are complex and diverse, and is a result of combination of factors. In terms of landslide susceptibility assessment and risk assessment, the influence of the factor interactions should be fully considered. In addition to the eight key impact factors mentioned in this study, there are some other factors proposed by other researchers, such as extreme rainfall events [39-40], land cover (standardized difference index NDVI and Vegetation type) [32], human activities (population density, road density) and other factors also have an impact on the spatial distribution of landslides, but not the main influencing factor. We cannot quantify these factors, and we need more sufficient data, which is an area for further research. There are many factors involved in the distribution of landslides, and their formation is complex.

7. Conclusion

XRA is a relatively developed area of landslides, which are controlled by various factors. In this paper, we identified 161 landslides in the area and investigated their distributions and their relationships to the influential factors of topography, geological environment, rainfall, seismicity and reservoir water. The following conclusions were obtained:

(1) The spatial distribution of landslides in XRA shows significant regional differences in the macro, and the main influencing factor is stratigraphic lithology. O-S strata have the longest distribution section and the largest number of landslides; Z-∈ have the highest distribution density, which is a landslide-prone formation, so these two types of strata have the greatest impact on landslides. The influence of lithological conditions on landslides is mainly the rock with weak structural layers. Especially in Baitieba Township-Huanghua Town section, the distribution of landslides varies greatly. This section is dominated by clastic group and carbonate group, while the landslides are distributed in clastic group. Landslide density is the highest in metamorphic group. The number of landslides is the largest in clastic group, and it is a typical group prone to develop landslides. So, these two types of groups have the greatest influence on the distribution of landslides.

(2) The landslides are mostly distributed in the area with an elevation of 600~1200 m, slopes of 10°~40°, O-S strata, within 4 km from the fault, average annual rainfall of 800~900 mm and PGA of 0.15 g.

(3) The landslide resurrection induced by reservoir water was most significant when the first impoundment reached 540 m, and then gradually weakened with the annual deformation and stress adjustment of the landslide. There are 53 landslides affected by reservoir water changes, and reservoir water changes in the front part of most of the wading landslides. The landslide developed in clastic group mainly composed of thin-to-layered sandstone, siltstone, mudstone, and shale. The mudstone and shale interlayers are prone to soften under the action of reservoir water, resulting in a significant

reduction in shear strength of the weak structural layer and local deformation and failure. Therefore, it is necessary to focus on wading landslides controlled by weak strata.

(4) Individual factors such as elevation, slope, aspect, lithology, fault, rainfall and seismicity are related to the spatial distribution of landslides. Individual factor is weak in the ability to explain the spatial distribution of landslides, while factor interactions are strong. The interactions between lithology and elevation, seismicity and faults can explain more than 30% of the spatial distribution of the landslides. The interaction between lithology and rainfall can explain the 45.9% spatial variation of landslides, indicating that it has the greatest influence on the spatial distribution of the landslide. For the section of Baitieba Township-Huanghua Town, not only average annual rainfall is large, but the distribution of weak strata is wide. So landslide density is the highest.

References

[1] ICOLD 2002 *Reservoir Landslides: Investigation and Management—Guidelines and Case Histories* (Paris: International Commission of Large Dams Publications) p 124
[2] Veveakis E, Vardoulakis I and Di Toro G 2007 *J Geophys Res-Earth* 112 1-21
[3] Iqbal J, Dai F, Hong M, Tu X and Xie Q 2018 *J. Earth Sci.* 29 646-661
[4] Liao Q L, Li X, Li S D and Dong Y H 2005 *Chinese Journal of Rock Mechanics and Engineering* 24 3146-3153
[5] Wu X L, Zhan F B, Zhang K X and Deng Q L 2016 *Environ. Earth Sci.* 75 1-16
[6] Wang Z W, Yang J, Zhang B J and Ma S S 2004 *Rock and Soil Mechanics* 25 1837-1840
[7] Liu X X, Xia Y Y, Lian C and Zhang K P 2005 *Rock and Soil Mechanics* 26 1427-1431
[8] Deng J H, Wei J B, Min H, Tham L G and Lee C F 2005 *Science In China Series E-Engineering & Materials Science* 48S 27-32
[9] Wang F, Zhang Y, Huo Z, Peng X, Araiba K and Wang G 2008 *Landslides* 5 321-329
[10] Riemer W 1992 *Landslides and Reservoirs (Keynote Paper)* (Christchurch: Researgate) 3 1373-2004
[11] Wang F W, Zhang Y M, Huo Z T, Matsumoto T and Huang B L 2004 *Landslides* 1 157-162
[12] Deng J H, Ma S S, Zhang B J and Wang Z W 2003 *Chinese Journal of Rock Mechanics and Engineering* 22 1730-1737
[13] Niu Z 2015 *Landslide stability analysis of Yalong River Ertan Hydropower Station reservoir area* (Chengdu: Southwest Jiaotong University)
[14] Liu G R 2007 *Study on stability and Engineering Impact of Jinjiang Landslide* (Chengdu: Chengdu University of Technology)
[15] Liu S Y and Li P F 2018 *Chinese Journal of Underground Space and Engineering* 14 1393-1399
[16] Jian W X, Wang Z J and Yin K L 2009 *Eng. Geol.* 108 86-95
[17] Xia M, Ren G M and Ma X L 2013 *Natural Hazards* 68 467-482
[18] Bai S B, Wang J, Lü G N, Zhou P G, Hou S S and Xu S N 2010 *Geomorphology* 115 23-31
[19] Miao H B, Wang G H, Yin K L, Kamai T and Li Y Y 2014 *Eng. Geol.* 171 59-69
[20] Deng Q L, Fu M, Ren X W, Liu F Z and Tang H M 2017 *Eng. Geol.* 221 170-183
[21] Fan Z J and Wang Z 2013 *The Chinese Journal of Geological Hazard and Control* 24 38-43
[22] Yin Y P, Huang B L, Wang S C and Li J H 2015 *Environ. Earth Sci.* 73 3187-3196
[23] Grilli S T and Watts P 2005 *J. Waterw. Port Coast.* 131 283-297
[24] Chen Y Z and Dai F C 2018 *Industrial Construction* 48 634-639
[25] Zhu J and Tang C 2012 *Remote Sensing Technology and Application* 27 458-464
[26] Zhuo B X 2011 *Remote Sensing Interpretation & Application of Geology Engineering* (Beijing: China Railway Publishing House) p 1-742
[27] Dai F C and Tu X B 2013 E*valuation of reservoir bank stability of Xiluodu Hydropower Station on Jinsha River* (Beijing: Institute of Geology and Geophysics, Chinese Academy of Sciences) p 13-126
[28] Quantin C, Allemand P and Delacourt C 2004 *Planet. Space Sci.* 52 1011-1022
[29] Xu C, Xu X W, Yao X and Dai F C 2014 *Landslides* 11 441-461

[30] Wang J F, Li X H, Christakos G, Liao Y L, Zhang T, Gu X and Zheng X Y 2010 *Int. J. Geogr. Inf. Sci.* 24 107-127
[31] Luo W, Jasiewicz J, Stepinski T, Wang J F, Xu C D and Cang X Z 2016 *Geophys. Res. Lett.* 43 692-700
[32] Lin L, Lin Q G and Wang Y 2017 *Nat. Hazard. Earth Sys.* 17 1411-1424
[33] Deng H Y and Wang C H 2011 *China Soil and Water Conservation* 5 63-66
[34] Broothaerts N, Kissi E, Poesen J, Van Rompaey A, Getahun K, Van Ranst E and Diels J 2012 *Catena* 97 127-136
[35] Guo C B, Montgomery D R, Zhang Y S, Wang K and Yang Z H 2015 *Geomorphology* 248 93-110
[36] Yin H, Hu F S, Sui S Y and Du L X 2010 *Journal of Arid Land Resources and Environment* 24 138-144
[37] Dai F C and Lee C F 2002 *Geomorphology* 42 213-228
[38] Qi S W, Xu Q, Lan H X, Zhang B and Liu J Y 2010 *Eng. Geol.* 116 95-108
[39] Wang Y Q and Zhou L 2005 *Geophys. Res. Lett.* 32
[40] Zhai P M, Zhang X B, Wan H and Pan X H 2005 *J. Climate* 18 1096-1108